Photochlorination of Propane

ALBERTO E. CASSANO and J. M. SMITH

University of California, Davis, California

The chlorination of propane was studied in a tubular flow reactor, with outside illumination, at atmospheric pressure. At chlorine concentrations of less than 1.5 mole % (and inert nitrogen above 94%) a second-order (in chlorine) rate expression was indicated. At higher chlorine or propane concentrations propane affects the rate. Two rate equations, based upon different termination steps for the chain carriers, were found to fit the data. For the low concentration region the apparent activation energy for the overall reaction was 3.4 kcal./g.-mole. Most of the measurements were carried out with polychromatic light, but data taken with a narrow band of radiation, over the range 2,200 to 5,400Å, showed an increase in rate with decreasing wave length. As a first step toward reactor design, differential reactor data were used to predict the conversion for laminar flow, integral reactor conditions. A reactor model which included the effects of residence time distribution and radial variation in light intensity gave good agreement with experimental data. A plug-flow model was less satisfactory.

The impetus for this work was an earlier study (*1*) on the same reaction at low chlorine concentrations. To understand the objectives of the present study it is necessary to mention the earlier results. In that work kinetic constants were determined for the photochlorination of propane in a differential, tubular flow reactor operated at 30°C. and at atmospheric pressure. Chlorine concentrations were maintained below 1.0 mole % by dilution with nitrogen, and an excess of propane was present. The rate of disappearance of chlorine closely fit the following equation:

$$-\Omega_{Cl_2} = k_{o,\lambda}\,(Cl_2)^2 \qquad (1)$$

where k_o is a function of wavelength and the local light intensity at a radial position r in the reactor:

$$k_{o,\lambda} = K_\lambda\, I_{r,\lambda}\, \alpha_\lambda \qquad (2)$$

Polychromatic light, directed radially into the reactor, was used and a single value of the rate constant K was obtained for the range 2,200 to 5,400 Å. The light intensity was varied with filter solutions that had different transmission coefficients θ_λ but which gave essentially the same spectral distribution of transmitted radiation. Thus the intensity at the inside wall of the reactor for radiation in one direction is $I_{w,\lambda}\,\theta_\lambda$ where $I_{w,\lambda}$ is the value without filters. The absorptivity of chlorine at low concentrations is small so that the intensity at any radius of the total radiation from both directions is given by

$$I_{r,\lambda} = \frac{2R}{r}\, I_{w,\lambda}\, \theta_\lambda \qquad (3)$$

By assuming no radial concentration gradient and summing over the wave length range, the average rate across the reactor is

$$-\bar{\Omega}_{Cl_2} = k_o\,(\overline{Cl_2})^2 \qquad (4)$$

Then an average intensity $\overline{I}_\lambda$ can be used in Equation (2). Integration of Equation (3) from 0 to R to obtain $\overline{I}_\lambda$ and summation of Equation (2) over the wavelength range give the final expression for average values of k_o and K:

$$k_o = 4K\sum_\lambda (I_{w,\lambda}\,\theta_\lambda\,\alpha_\lambda) = 4K\sigma \qquad (5)$$

The details of the derivation are given in reference *1*. The quantity σ is introduced here as a measure of the light absorbed by the reaction mixture, and hence determines the rate of the primary step in the photochemical process. It will be termed the specific rate of energy input.

It is well understood (*2, 3*) that rates for photochemical reactions may be a function of wavelength, although predictions of the effect have yet not been successful (*4*). Variations of quantum yields with wavelength for actinometer reactions (*5* to *9*) are examples. One objective of the present study was to measure rate constants vs. λ under the mild chlorinating conditions where Equations (1) and (2) are valid.

Equations (1) and (2) are based upon a stationary state development, with a first-order termination step of propyl radicals assumed, either homogeneously or heterogeneously at the reactor wall. The type and importance of the termination step in a chain reaction have a marked effect on the overall rate. Also concentration levels can influence the termination steps. Hence new data were obtained at higher chlorine concentrations (maintaining a fourfold excess of propane) to determine if the conditions upon which Equations (1) and (2) are based are satisfactory over a wide range of concentrations.

The complexity of design of photoreactors will be strongly dependent on the apparent activation energy for the overall reaction. In chain reactions the activation energy of the termination steps acts so as to reduce the overall value. There are experimental and theoretical studies (*10* to *12*) indicating that E is very low. If E is small enough, the energy and mass balances are not coupled and can be solved independently. A third goal of the present work was to evaluate the activation energy for the photochlorination of propane.

The final use of differential photoreactor data is for scale-up to larger reactors and conversions. A test of longitudinal scale-up was carried out by measuring first conversions for laminar flow, long reactors. These results were then compared with conversions predicted with Equations (1) and (2) and reactor models based upon plug-flow and parabolic velocity profiles.

Alberto E. Cassano is on leave from the Facultad de Ingenieria Química, Santa Fe, Argentina.

APPARATUS

The apparatus was the same as described previously (*1*) except for minor changes designed to improve accuracy. The same reactor (optically clear, fused quartz) 0.2 cm. I.D. and 0.4 cm. O.D., and jacket, 1.6 cm. I.D. and 1.8 cm. O.D., were used. However, the system was operated both as a differential and as an integral reactor in the present work. The lamp was a 360-w. General Electric UA-3, medium pressure, mercury arc with characteristics described in reference *1*.

In the present work the maximum length of irradiated reactor was 10.0 cm. Since the lamp arc length was 15.2 cm., end effects due to nonuniform radiation in the axial direction were negligible. More accurate flow rate measurements for nitrogen were obtained by using a soap film meter, and the chlorine flow rate was held more nearly constant by installing in series a second differential-pressure flow controller. A third change was the use of a higher capacity circulating pump for the jacket fluid, thus reducing the temperature difference between inlet and outlet of the jacket to less than 1°C.

In the actinometer runs designed to measure the light intensity, distilled degassed water was pumped through the reactor jacket. For the chlorination runs, filter solutions were used.

EXPERIMENTAL PROCEDURE

Actinometer runs were made after every 100 hr. of lamp operation to have an accurate knowledge of the decay characteristics of the lamp. For these runs the feed consisted of an aqueous solution of 0.05 molal oxalic acid and uranyl sulfate, 0.01 molal, at 30°C. The conversion was maintained between 5 and 15%. Details of operating procedures and special precautions are given elsewhere (*1, 2, 13*).

The general chlorination procedures were as described in reference *1*. Ninety minutes were generally necessary to stabilize the system prior to making measurements. Sample collection periods were 10 min. or more to increase the accuracy of the chemical analyses. After each chlorination run a dark-reactor run was made to evaluate the chlorine flow rate by analysis and to check the presence of dark reaction. The period of continuous lamp operation was limited to 14 hr., after which a standard cleaning procedure (*1*) was employed to clean the reactor walls. After each cleaning, long purge times with reactants at normal rates were used to restabilize the system. By this procedure reproducibility of data within a few percent was possible. Samples of the filter solutions were analyzed for changes in transmission coefficients every 2 hr. with a Beckman DB Spectrophotometer.

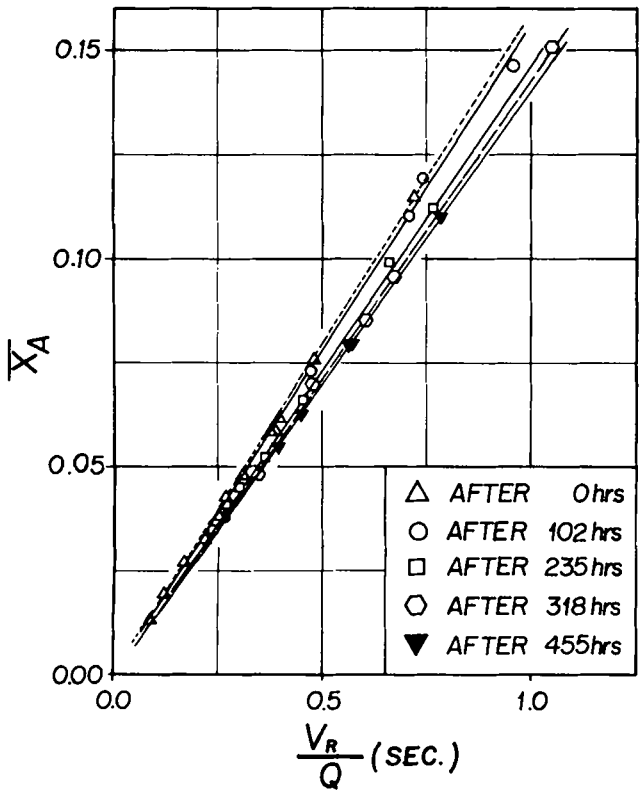

Fig. 1. Actinometer results.

Several operating procedures specific for this study were needed. First, to study the effect of spectral distribution of the light, different filter solutions were used in the reactor jacket to block regions of emission of the lamp. Quantitative transmission coefficients of the various solutions over the required temperature and wavelength ranges were measured in a Cary Model 14 Spectrophotometer with a photometric accuracy better than 0.005 in the absorbance range used. Second, to operate at high chlorine concentrations, reproducibility tests were necessary every 8 hr. because of the possibility of wall deposits.

SCOPE AND PRECISION OF DATA

The range of operating conditions was:

Flow rate: N_{Re} = 300 to 1,750

Feed composition (mole %):

Nitrogen = 15 to 96%

Propane = 3.5 to 80%

Chlorine = 0.4 to 14%

Reactor length: 1.31 cm. for differential reactor runs, 10.0 cm. for integral reactor runs

Total range of wavelength: 2,200 to 5,400 Å.

Light intensity: Specific rate of energy input σ = (0.14 to 4.1) × 10^{-2} Einsteins/(sec.)(g.-mole)

Temperature: 27° to 52°C.

By careful control of flow rates, temperatures, lamp operation, and analysis methods, the mass balances on chlorine, when the irradiated and dark reactor runs were compared, agreed within 2%. Light intensities were believed to be accurate within 4% as determined by actinometer measurements and transmission characteristics of the filter solutions. Photochemical measurements are very difficult to duplicate quantitatively because of many poorly understood variables. It is possible however to put limits on reproducibility of results obtained in one laboratory. The final results involving all the measurements are the kinetic constants, and it is believed that the values reported here are reproducible within 10%.

It is appropriate to emphasize that unusual precautions are necessary to obtain satisfactory photochemical rate data, particularly for flow systems where cleaning conditions are sometimes difficult. It has been our experience that reproducibility requires strict adherence to precise conditions of preparation, operation, and cleaning of the system. Furthermore, long periods are required prior to measurements, even for apparently homogeneous reactions, to ensure steady conditions of flow temperature, lamp operation, and wall behavior.

ACTINOMETER STUDIES

The intensity at the inside wall of the reactor was obtained (see reference *1*) by measuring the conversion $\bar{x}_A$ of oxalic acid by photochemically excited uranyl ions. It can be shown that $\bar{x}_A$ is related to the rate $\bar{r}_A$ of this zero order reaction by the expression:

$$\bar{x}_A = \frac{(\bar{C}_x)_o - (\bar{C}_x)_L}{(C_x)_o} = \frac{-\bar{r}_A}{(C_x)_o}\frac{V_R}{Q} \qquad (6)$$

According to Equation (6) the experimentally determined conversion should be a linear function of V_R/Q with a slope proportional to $\bar{r}_A$. The data are plotted in this manner in Fig. 1, for each set of runs, and show a small but consistent decrease in slope with time. This decrease is due to the slow decay in output of the lamp. Data from Figure 1 giving the rate of reaction at various times are

Table 1. Decay of Lamp Output with Time
Total time of operation approx. 500 hr.

Run No.	Approx. lamp operating time, hr.	$\bar{r}_A \times 10^6$ (exp.) g.-moles/(sec.)(cc.)	$\bar{r}_A \times 10^6$ interpolated at time shown	$(I_w)_{tot} \times 10^8$ Einsteins/(sec.)(sq. cm.)	Observations
A-1 to A-12	0	7.79			
	51		7.68	1.48	Used with data on effect of wavelength
A-13 to A-18	102	7.56			
	168		7.52	1.45	Used with data showing effect of temperature
A-19 to A-24	235	7.47			
	276		7.34	1.42	Used with first 16 runs at high chlorine concentration
A-25 to A-30	318	7.19			
	386		7.16	1.38	Used with last 30 runs at high chlorine concentration
A-31 to A-36	455	7.00			
	475		7.00	1.35	Used with scale-up data

shown in column 2 of Table 1. Interpolated values at times corresponding to the chlorination measurements are given in column 3. The intensity can be ascertained from $\bar{r}_A$ and the characteristics of the lamp according to the equation developed in reference 1:

$$I_{w,t} = \frac{-\bar{r}_A R}{2 \sum_\lambda \left\{ \Phi_\lambda \frac{F_\lambda}{F_t} [1 - \exp(-2R\mu_\lambda)] \right\}} \quad (7)$$

Values of the quantum yield Φ_λ for the actinometer reaction and F_λ/F_{tot} for the lamp were reported in reference 1. The values of F_λ/F_{tot} from the lamp manufacturer are estimated to have an accuracy of 2 to 3%. The results for $I_{w,t}$ calculated from Equation (7) are given in Table 1. These intensities, taken at the appropriate time, were used in the analysis of the several types of chlorination data described in the last column of the table. A better actinometer system would be one that had the same adsorptivity as that for the chlorination mixture. When such a system is developed it should be possible to evaluate the accuracy of intensity values calculated from the oxalic acid actinometer by using Equation (7). Any errors in I_w obtained in this work would affect the absolute values of the rate constants for the chlorination reaction, but not their relative values.

The actinometer measurements were normally made with distilled degassed water in the reactor jacket. Since the chlorination data were always obtained with filter solutions in the jacket, the actinometer I_λ values were multiplied by the transmission coefficient θ_λ measured with the spectrophotometer. To test this procedure, one set of actinometer runs was carried out with a filter solution in the jacket. The experimental conversions were compared with computed values of $\bar{x}_A$ calculated by combining Equations (6) and (7) to eliminate $\bar{r}_A$. The resultant expression, after introducing the transmission coefficient θ_λ, is

$$\bar{x}_A = \frac{I_{w,t}\, \pi RL}{2(C_x)_o Q} \sum \theta_\lambda \Phi_\lambda \frac{F_\lambda}{F_t} [1 - \exp(-2R\mu_\lambda)] \quad (8)$$

The conversions computed from Equation (8) are compared with the experimental values in Figure 2. The agreement is good for these conditions but it is interesting to note that the predicted values with transmission coefficients used, determined spectrophotometrically for the filter solutions, are consistently larger. It may be that the deviation is due to successive reflections of light through the jacket. These reflections would have a different effect on $I_{w,\lambda}$ depending upon whether the jacket contained filter solution or distilled water While the effect is very small in this work, with more optically dense filter solutions or a lower optical efficiency for the reactor lamp system (see reference 1), it could be significant.

CHLORINATION STUDIES: EFFECT OF WAVELENGTH

To study the effect of wavelength on the overall rate constant, chlorination runs were made with three different filter solutions in the reactor jacket. These aqueous solutions of $Fe_2(SO_4)_3$ and $(NH_4)_2SO_4$ (filter No. 1), $Cu(NO_3)_2$ (filter No. 2), and $NiSO_4$ (filter No. 3) were chosen so as to transmit a narrow range of wavelength in each of three regions of strong emission of the lamp. The characteristics of the light reaching the inside wall of the reactor, after passing through the filter, are summarized in Table 2. The key rows in this table are No. 2, the specific rate of energy input σ, and No. 3, the principal wavelength range. Other rows in the table give the fraction of the light absorbed in the principal wavelength range, and the energy in kcal./g.-mole associated with the principal wavelength range.

Eight chlorination runs were made in each wavelength range with flow rates from 6 to 23 cc./sec. (at reactor conditions), chlorine concentrations from 0.4 to 1.67 mole %, a reactor length of 13.1 mm., and at 30°C. The rates calculated from these differential reactor runs agreed with the rate equation [Equations (1) and (2)] derived in reference 1. The slope of the rate vs. concentration lines shown in Figure 3 verifies the second-order dependency. The displacement of the lines is due to changes in σ and

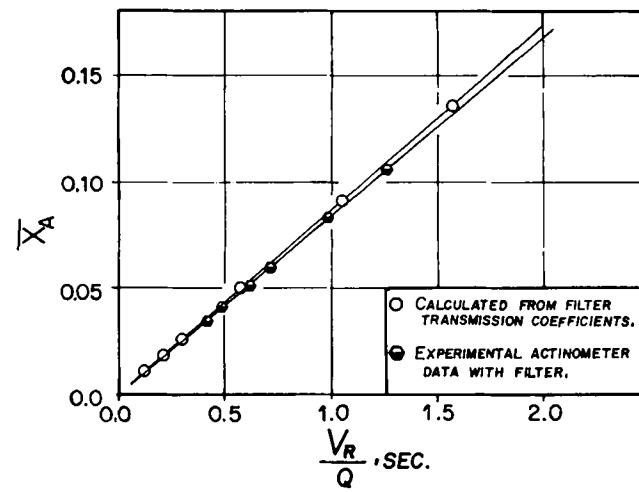

Fig. 2. Actinometer test of transmission characteristics of filter solution.

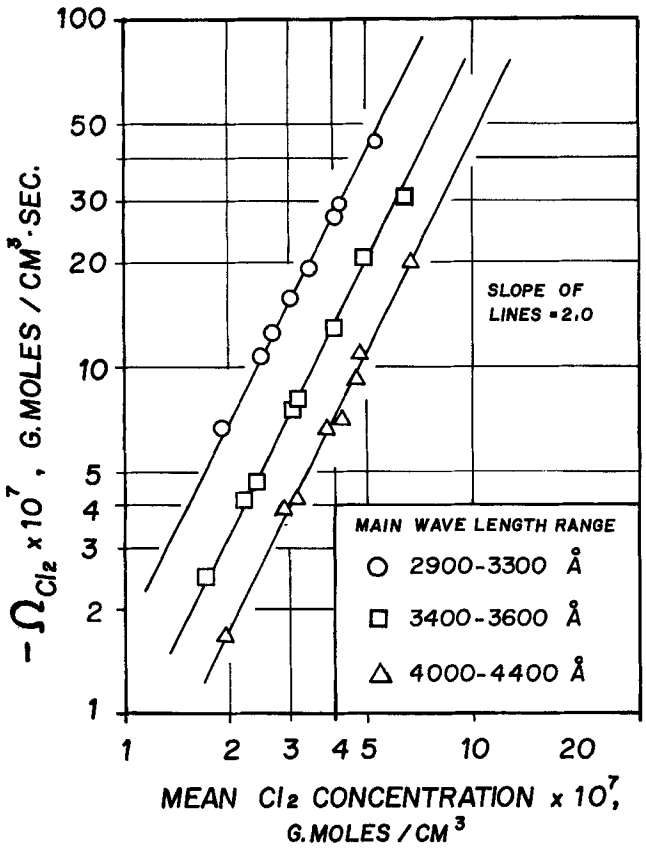

Fig. 3. Effect of concentration on reaction rate.

K with wavelength. To establish quantitatively the effect of λ on K, values of K were calculated by substituting Equations (4) and (5) in the mass balance equation for chlorine:

$$-\bar{v}_z \frac{d[\bar{Cl}_2]}{dz} + \bar{\Omega}_{Cl_2} = 0 \qquad (9)$$

The justification for Equation (9), where $\bar{v}_z$ is the average velocity, is discussed in reference *1*. Integration of Equation (9) and solution for K give

$$K = \frac{Q \quad \bar{x}_f}{V_R [Cl_2]_o (4\sigma)(1-\bar{x}_f)} \qquad (10)$$

where

$$\sigma = \sum_\lambda (I_{w,\lambda}\, \theta_\lambda\, \alpha_\lambda) = I_{w,t} \sum_\lambda \left(\frac{F_\lambda}{F_t}\, \theta_\lambda\, \alpha_\lambda\right) \qquad (11)$$

K values computed in this way are somewhat more accurate than those obtained by calculating $k_{o,\lambda}$ from Equation (4) and the data in Figure (3), and then K from Equation (5).

The results are summarized in Table 3, where the runs exhibiting the maximum deviation in K_λ (for a given wavelength range) are shown as well as the average value for each set of eight runs. A definite increase in K_λ with decreasing wavelength is observed in the average values. Note that the effect of wavelength on absorptivities of chlorine and filter solutions, as well as on the emission of the lamp, has been taken into account (through σ) prior to evaluating K. There is considerable information in the literature (*14* to *16*) indicating a variation in quantum yield and even product distribution with wavelength of radiation, presumably due to a variation in efficiency of the primary process. It has been postulated (*4, 14, 16*) that this effect on the primary process is related to the excess of energy over that needed to dissociate the absorbing molecule into activated atoms. The data of this study agree with this postulate. The primary process is

$$Cl_2 + h\nu \rightarrow 2\,Cl^* \qquad (12)$$

where the energy of radiation depends upon the frequency ν, and is given in row No. 7 of Table 2. The dissociation energy of chlorine is 57 kcal./g.-mole. A plot of the excess energy vs. K, Figure 4, indicates a linear relationship. The data available for Figure 4 are limited in extent and the total variation in K is not great (45%). However, it is believed that the accuracy of the data is good enough to attach significance to the progressive increase in K with decrease in wavelength.

The absolute value of K, averaged for the three wavelength regions, is about 50% less than the polychromatic K determined in the earlier work (*1*). The explanation for this difference is difficult to pinpoint, although the problems in reproducing kinetic results in photochemical studies made at different times are well known. The results reported here were obtained in the same apparatus used earlier but some operating procedures were different. The nitrogen used was 99.99% pure but did not carry the specification of less than 8 p.p.m. of oxygen which characterized the nitrogen used in reference (*1*). The severe inhibiting effect of oxygen even in small concentrations could account for the decrease in K. The soap

Table 2. Wavelength Characteristics of Light at Inside Wall of Reactor

Property	Filter 1	Filter 2	Filter 3
1. Total wavelength range of transmission, Å.	3,700 to 5,000	3,300 to 5,000	2,300 to 5,000
2. σ, Einsteins/(sec.) (g.-mole)	$0.141\ 10^{-2}$	$2.23\ 10^{-2}$	$4.04\ 10^{-2}$
3. Principal wavelength range, Å.	4,000 to 4,400	3,400 to 3,700	2,900 to 3,300
4. $\frac{\sigma \text{ for principal range}}{\sigma \text{ for total range}}$	0.85	0.85	0.78
5. Principal emission lines in the principal range	4,358	3,654	3,022 to 3,131
6. $\frac{\text{Approximate } \sigma \text{ for principal line}}{\sigma \text{ for total range}}$	0.63	0.77	0.70
7. Energy in kcal./g.-mole for an approx. mean value of (3)	66.5	78.6	92.2
8. Energy in excess of dissociation energy of chlorine, kcal./g.-mole	9.5	21.6	35.2

TABLE 3. EFFECT OF WAVELENGTH ON REACTION RATE

Run No.	Main wavelength range, Å.	$\sigma \times 10^2$, Einsteins/(sec.)(g.-mole)	N_{Re}	Q, cc./sec.	$(Cl_2)_o$ mole %	Propane mole %	x_{Cl} %	K_λ, cc./Einstein
λ-1	4,000		303	6.96	0.97	5.83	1.05	0.82×10^9
λ-5	to	0.141	491	11.70	1.16	3.43	0.70	0.76×10^9
Ave.	4,400		—	—	—	—	—	0.79×10^9
λ-10	3,400		730	17.13	1.64	4.39	11.50	0.92×10^9
λ-14	to	2.23	943	22.45	1.22	3.35	7.60	1.01×10^9
Ave.	3,700		—	—	—	—	—	0.96×10^9
λ-19	2,900		730	17.13	1.35	4.51	19.70	1.17×10^9
λ-21	to	4.04	950	22.62	0.77	3.30	9.0	1.10×10^9
Ave.	3,300		—	—	—	—	—	1.14×10^9

Reactor length = 13.1 mm.; temperature = 30°C.

flow meter employed in the nitrogen stream for the present work, even though followed by a silica gel adsorber, could give a slightly different water concentration in the reactants stream. Here again concentration changes in the low parts per million range could affect homogeneous processes and wall stabilization phenomenon, both of which can be important in reproducing chain reaction kinetics.

CHLORINATION STUDIES: EFFECT OF TEMPERATURE

The objective of this part of the work was to evaluate the apparent activation energy and frequency factor for the overall chlorination process. Hence it was necessary to operate at low chlorine concentrations where Equations (4) and (5), or (10), were known to represent the rate satisfactorily. Rates were measured under differential reactor conditions with a filter solution which gave approximately the same spectral distribution of transmitted light as in the previous work (2). The filter solution allowed significant transmission from 2,600 to 4,600 A.

To use Equation (10) to calculate K it was necessary to take into account the effect of temperature on the absorptivity α_λ of chlorine, and on the transmission θ_λ of the filter solution. The data of Gibson and Bayliss (17) were used to establish the first effect. In our temperature range (27° to 52°C.) the variation of α_λ was less than 2% in the main range of absorption but up to 20% at the extreme wavelengths. The second effect is much more important and it was necessary to measure θ_λ at four temperatures, 27.5°, 32°, 41.5°, and 49°C., over the entire wavelength range. Figure 5, on semilog coordinates, illustrates the magnitude and specific nature of the effects for different wavelength regions.

The K values and a least-mean-square line fitted to the data are shown in Figure 6. An activation energy of

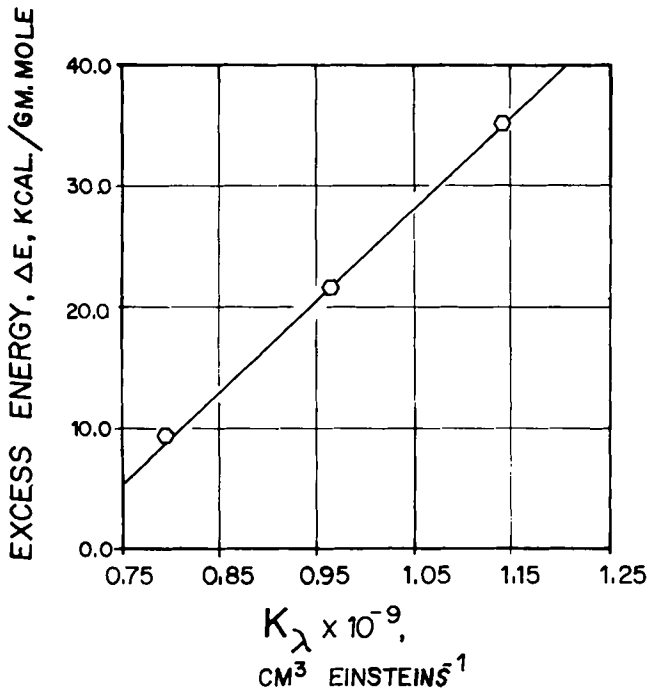

Fig. 4. Effect of wavelength on reaction rate constant.

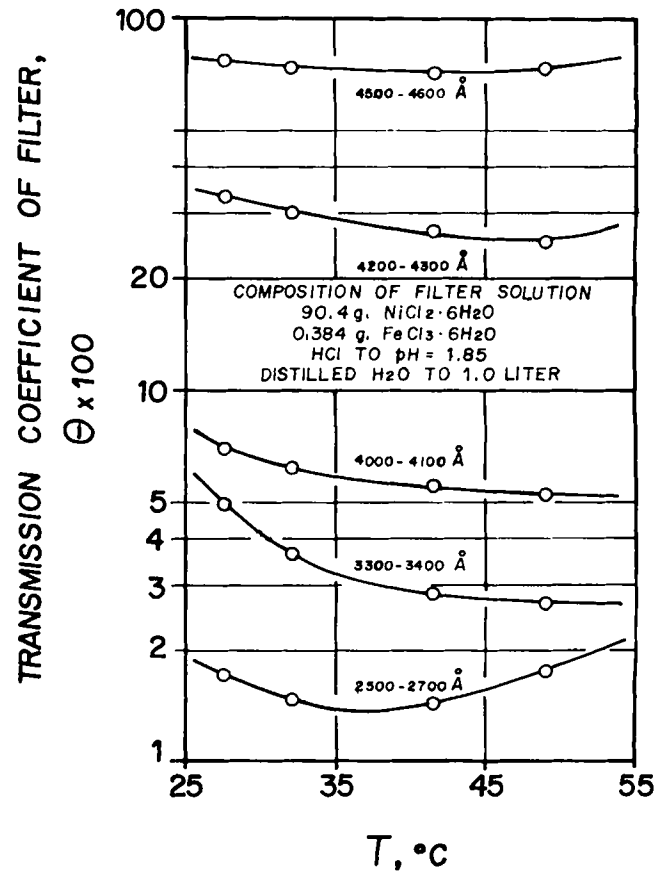

Fig. 5. Effect of temperature on opacity of filter solution.

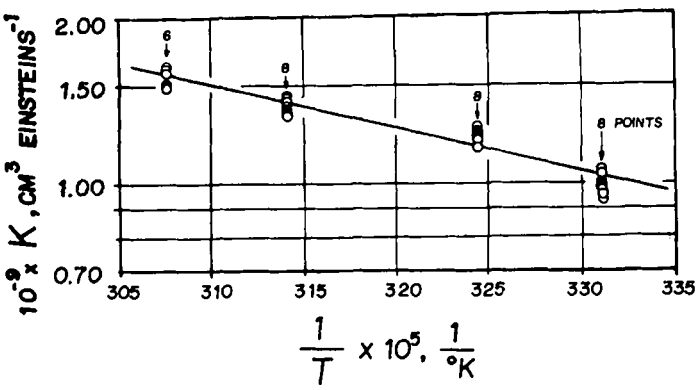

Fig. 6. Arrhenius plot of rate vs. temperature data.

3.4 ± 0.5 kcal./g.-mole is indicated, according to the expression:

$$K = Ae^{-E/R_gT} = 0.29 \times 10^{12} \exp\left(-\frac{3.37}{R_gT}\right) \quad (13)$$

Approximate magnitudes of activation energies and frequency factors for gas phase monochlorination of light hydrocarbons photochemically have been estimated in the literature (*10, 18*) and range from 10^9 to 10^{12} and 0 to 4 kcal./g.-mole. These magnitudes were obtained by assuming mechanisms for the reactions and combining A and E for the individual steps. Equation (13) supplies specific values, and it is interesting to note that they fall within the estimated range. Apparent activation energies of 6 and 9 kcal./g.-mole have been measured (*19, 20*) for liquid phase chlorination of C_7H_{16} and $C_{16}H_{34}$, respectively.

EFFECT OF CONCENTRATION: RATE AT HIGH CONCENTRATIONS

Equations (1) and (2) were derived (*1*), with the assumptions that the concentrations of Cl° and Pr° were small (stationary state hypothesis), from the following mechanism:

$$Cl_2 + h\nu \rightarrow 2Cl^\circ\ ;\ \Omega = 2k_{1,\lambda}\,\alpha_\lambda\,(Cl_2)I_\lambda \quad (14)$$

$$Cl^\circ + PrH \rightarrow Pr^\circ + HCl;\ \Omega = k_2\,(Cl^\circ)(PrH) \quad (15)$$

$$Pr^\circ + Cl_2 \rightarrow PrCl + Cl^\circ;\ \Omega = k_3\,(Pr^\circ)(Cl_2) \quad (16)$$

$$Pr^\circ \rightarrow \text{end product};\ \Omega = k_4\,(Pr^\circ) \quad (17)$$

Equations (14), (15), and (16) are used customarily to describe the primary and propagation steps in photochlorination and have some experimental verification as discussed by Calvert and Pitts (3). The rate Ω in Equation (14) is written for a narrow wavelength range and the sequence is based upon the deactivation of Pr° as the controlling termination process. Since a first-order termination step is likely to be heterogeneous (*11, 20A*), k_4 depends upon the radius of the reactor:

$$k_4 = \frac{2k_{w4}}{R} \quad (18)$$

In terms of the individual rate constants, the form of Equation (1), which results from analyzing the stated mechanism, is

$$-\Omega_{Cl_2} = \frac{2k_1\,k_3}{k_4}\,(I_{r,\lambda}\,\alpha_\lambda)\,(Cl_2)^2 \quad (1A)$$

or

$$-\Omega_{Cl_2} = K\,I_{r,\lambda}\,\alpha_\lambda\,(Cl_2)^2 = k_{o,\lambda}\,(Cl_2)^2 \quad (1B)$$

This expression explains accurately data at chlorine compositions less than 1.5 mole % and in dilutions with nitrogen of 94% or more. The question arises: would Equation (*1A*) explain rate data at higher chlorine and propane concentrations where the large concentration of nitrogen does not exist?

To investigate this situation experimentally σ was reduced to retain differential reactor operation at high chlorine. The final runs were made at $\sigma = 0.348 \times 10^{-2}$ Einsteins/(g.-mole)(sec.) with most of the energy in the 2,900 to 3,700 and 4,200 to 4,400 Å. ranges. The formation of wall deposits increases with chlorine and σ (see reference *1*). Runs were made over a 12-hr. period at 8 and 14 mole % chlorine level. Samples taken every 90 min. gave the same analysis within 5% and no trend was observed. Apparently σ was low enough to prevent deposits. Nevertheless, the final data were all taken with a maximum continuous operating time of 8 hr. between shutdown for cleaning. Runs were made with chlorine concentrations from 3.4 to 14 mole %, propane 37.3 to 79.7 mole %, and nitrogen 15.1 to 65.4 mole %, all at 30°C. The ratio of propane to chlorine in the feed was set at 3.6 or more to prevent the formation of dichlorinated products, but the nitrogen-chlorine ratio was as low as 2.2. Essentially isothermal conditions were achieved.

ANALYSIS OF DATA

An initial examination of the rates $(-\Omega_{Cl_2})$, calculated on the basis of differential reactor operation, indicated that Equation (1A) was not suitable. The concentration of propane and/or nitrogen had a pronounced effect. The next step was to determine quantitatively the effect of propane and nitrogen by fitting the data to empirical rate equations of the form

$$-\overline{\Omega}_{Cl_2} = k_I\,(\overline{Cl}_2)^\alpha\,(\overline{PrH})^\beta \quad (19)$$

$$-\overline{\Omega}_{Cl_2} = k_{II}\,(\overline{Cl}_2)^{\alpha'}\,(\overline{PrH})^{\beta'}\,(\overline{N}_2)^\gamma \quad (20)$$

By multiple regression analysis the least-mean square fit of the data gave the following results:

$$-\overline{\Omega}_{Cl_2} = 0.62 \times 10^7\,(\overline{Cl}_2)^{1.06}\,(\overline{PrH})^{1.13} \quad (21)$$

$$-\overline{\Omega}_{Cl_2} = 7.14\,(\overline{Cl}_2)^{1.01}\,(\overline{PrH})^{0.44}\,(\overline{N}_2)^{-0.51} \quad (22)$$

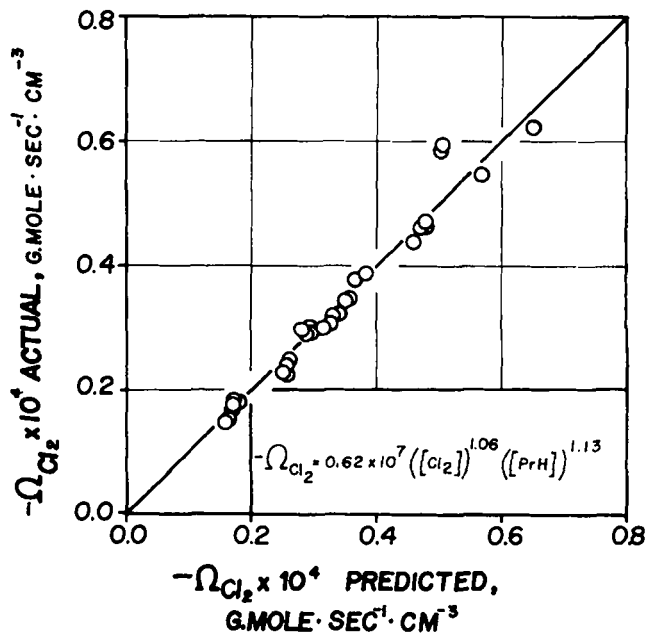

Fig. 7. Correlation of rate data according to Equation (21).

The agreement with the data is illustrated for Equation (21) in Figure 7 and for Equation (22) in Figure 8. The deviations between experimental and calculated rates are noted to be somewhat smaller for Equation (22).

The third step was to seek a reaction sequence analogous to Equations (14) to (18) which would approach the empirical expressions. The initiation and propagation processes were not likely to be different, but the high concentrations of chlorine and low concentration of nitrogen could affect the termination step. Two types of termination steps were found which would lead (with the stationary state assumption) to rate expressions similar to Equations (21) and (22). Attempts were unsuccessful to explain a rate expression involving only chlorine and nitrogen concentrations.

Mechanism I

If it is supposed that the only significant termination step is

$$Cl^{\bullet} \rightarrow \text{end}; \quad \Omega = k_5(Cl^{\bullet}) \tag{23}$$

the final rate equation is

$$-\Omega_{Cl_2} = \frac{2k_1k_2}{k_5}\,(\alpha_\lambda I_{r,\lambda})\,(Cl_2)\,(PrH) \tag{24}$$

which, for constant σ, can be developed to the form

$$-\bar{\Omega}_{Cl_2} = k_I\,(\overline{Cl_2})\,(\overline{PrH}) \tag{25}$$

This result is similar to empirical Equation (21). The first-order termination step [Equation (23)] is likely to be heterogeneous. Hence, the true rate constant k_{w5} at the wall of the reactor would be related to the equivalent homogeneous (based upon unit volume) constant k_5 by the expression

$$k_5 = \frac{2k_{w5}}{R} \tag{26}$$

Equations (1A) and (24) can be derived as special cases of a more general development which considers that termination steps for both Pr° [Equation (17)] and Cl° [Equation (23)] are significant. If $k_5/k_2 << 1/k_3$, the general equation reduces to Equation (1A), and if $k_4 << k_5k_3/k_2$, Equation (24) is obtained. If one or both of the termination steps were heterogeneous, changes in level of chlorine and propane could change the characteristics of the wall and therefore, k_{w4} and k_{w5}. This could explain the apparent change in rate equation from Equation (1A) to (24) as the chlorine and propane concentrations increase. Another explanation is that as chlorine increases the Cl° termination step [Equation (23)] becomes more important than the Pr° termination step [Equation (17)].

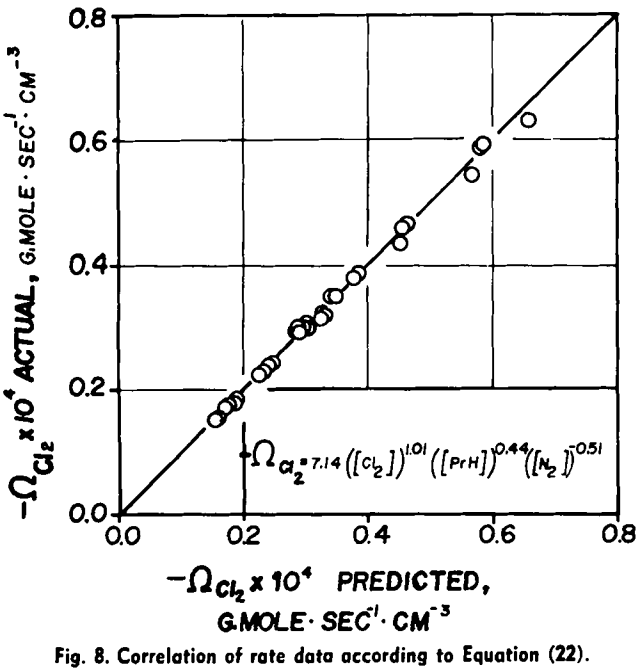

Fig. 8. Correlation of rate data according to Equation (22).

Mechanism II

An effect of nitrogen upon the rate can be introduced by supposing that the significant termination step is

$$Cl^{\bullet} + Pr^{\bullet} + N_2 \rightarrow PrCl + N_2 \tag{27}$$

$$\Omega = k_6\,(Cl^{\bullet})\,(Pr^{\bullet})\,(N_2) \tag{28}$$

A third body, in this case nitrogen, has been proposed by Steacie (*11*) as a means of stabilizing the reaction bebetween two atoms or free radicals. With the use of this reaction and the stationary state hypothesis, the rate equation is

$$-\Omega_{Cl_2} = \left(\frac{k_1\,k_2\,k_3}{k_6}\right)^{1/2} \frac{(\alpha_\lambda I_{r,\lambda})^{1/2}\,(Cl_2)\,(PrH)^{1/2}}{(N_2)^{1/2}} \tag{29}$$

For constant σ this can be converted to

$$-\bar{\Omega}_{Cl_2} = k_{II}\,(\overline{Cl_2})\,(\overline{PrH})^{1/2}\,(\overline{N_2})^{-1/2} \tag{30}$$

which is similar to empirical Equation (22). Since Equation (27) requires a third-order collision, it is difficult to imagine it to be a heterogeneous termination process. It is possible to derive a rate expression of the form of Equation (28) by supposing a reaction between adsorbed Cl° and Pr°, and nitrogen in the gas phase, but it appears to be improbable.

Evaluation of Rate Constants

The combined rate constants K_I and K_{II} were next evaluated to provide a quantitative test of Equations (24) and (29). These constants are defined as

$$K_I = \frac{2k_1\,k_2}{k_5} \tag{31}$$

$$K_{II} = \left(\frac{k_1\,k_2\,k_3}{k_6}\right)^{1/2} \tag{32}$$

The method was to convert Equations (24) and (29) to expressions for $-\bar{\Omega}_{Cl_2}$, sum over the wavelength range, and then substitute each result in the mass balance, Equation (9). The integrated result could then be used with the experimental conversion data to evaluate K_I and K_{II}. This is the same procedure as was used to establish K values from Equation (10) for the dilute chlorine data. However, at high chlorine the assumption of low optical density used in the derivation of Equation (10), see reference *1*, could introduce errors. To check this, the intensity equation was integrated with a finite, average value of $\overline{\alpha(Cl_2)}R$ and the result used to evaluate K_I and K_{II}. Comparison with the simpler solution, given in the next paragraph, indicated a difference of less than 4%. Hence the correction was not necessary.

Table 4. Illustrative Results for Mechanisms I and II

Run No.	N_{Re}	Q, cc./sec.	$(Cl_2)_o$, %	$(C_3H_8)_o$, %	$(N_2)_o$, %	x_{Cl_2}, %	$K_I \times 10^{-8}$ cc./(Einsteins)	$K_{II} \times 10^{-2}$ (g.-mole)$^{1/2}$ (sec.)$^{1/2}$ (Einsteins)$^{1/2}$	Observations
H-20	865	13.4	3.53	40.45	56.02	3.21	0.46	1.05	Run giving minimum K_I
H-39	937	8.6	5.18	79.72	15.10	13.40	0.65	1.10	Run giving maximum K_I
H-38	956	12.4	5.36	49.84	44.80	4.66	0.50	1.15	Run giving maximum K_{II}
H-45	954	9.8	7.74	68.32	23.94	8.29	0.52	1.03	Run giving minimum K_{II}
H-10	966	10.8	14.22	53.56	32.22	6.15	0.54	1.09	Randomly chosen
H-30	1,287	20.6	4.49	32.89	62.62	1.94	0.52	1.14	Randomly chosen
Average (46 runs)	—	—	—	—	—	—	0.53	1.10	Average

$\sigma = I_{w_i} \Sigma_\lambda \left(\theta_\lambda \alpha_\lambda \frac{F_\lambda}{F_t} \right) = 0.348 \times 10^{-2}$, Einsteins/(sec.) (g.-mole).
$L = 13.1$ mm.; $t = 30$°C.

For $\overline{\alpha(Cl_2)}\ R \to 0$, the expressions [analogous to Equation (10)] for K_I and K_{II} are

$$K_I = \frac{\bar{v}_z \int_o^{\bar{x}_L} \frac{d\bar{x}}{(1-\bar{x})\ (a-\bar{x})}}{4\sigma (Cl_2)_o L} \tag{33}$$

$$K_{II} = \left(\frac{b}{4\sigma} \right)^{1/2} \frac{\bar{v}_z}{L} \int_o^{\bar{x}_L} \frac{d\bar{x}}{(1-\bar{x})\ (a-\bar{x})^{1/2}} \tag{34}$$

where

$$a = \frac{(PrH)_o}{(Cl_2)_o} \tag{35}$$

$$b = \frac{(N_2)_o}{(Cl_2)_o} \tag{36}$$

Equations (33) and (34) were integrated numerically with the Newton-Cotes five-point formula with a step size (Δx) of 10^{-4}. Table 4 gives the results for K_I and K_{II} for several conditions: runs showing maximum and minimum values, results for randomly chosen runs, and the average values for the forty-six runs available. The best fit is obtained with mechanism II; the maximum deviation from the average value was 6.3%. For mechanism I the maximum deviation was 22%. Equations (24) and (29) show a different effect of σ so that data obtained with different light intensities would have been valuable in distinguishing between the two mechanisms. Unfortunately these experiments could not be performed, because at the end of the work the lamp output was no longer stable and the quart zreactor showed signs of loosing its transmissivity.

The results of Stauff (*20*) on the chlorination of $C_{16}H_{34}$ in CCl_4 solution agree with mechanism II. While no numerical values were given, he proposed, on the basis of batch reactor studies, an equation equivalent to

$$-\bar{\Omega}_{Cl_2} = k''(\bar{I})^{1/2}\ (Cl_2)\ (C_{16}H_{34})^{1/2} \tag{37}$$

In dilute solutions of $C_{16}H_{34}$ in CCl_4 the effect of (CCl_4) on the rate would be constant so that Equation (37) is similar to Equation (29). For low chlorine concentrations Stauff proposed

$$-\bar{\Omega}_{Cl_2} = k'''(\bar{I})\ (Cl_2)^2 \tag{38}$$

This is the same as Equation (1A) which described our experiments for dilute chlorine conditions.

LONGITUDINAL SCALE-UP MODEL STUDIES

The ultimate purpose of this section was to compare experimental conversions in a long reactor (100 mm.) with those predicted from rate data determined under differential reactor conditions. First it is desirable to compare models that may be used for the scale-up process. In particular it is of interest to investigate the effect of residence time distribution in laminar flow. For low conversions Denbigh (*21*) has shown the effect to be modest for a second-order reaction even when radial diffusion is neglected. For a photochemical tubular reactor, irradiated from outside, the intensity variation radially causes the rate of reaction to be higher near the center than near the outer tube wall. This, as well as radial diffusion, will tend to counterbalance the effect of the parabolic velocity profile on the conversion.

These facts suggest that a plug-flow model may be a good approximation. The situation was studied quantitatively for a photoreactor operating at conditions similar to those of our experimental work on the chlorination of propane at low chlorine. These conditions are:

1. Steady laminar flow with constant physical properties (isothermal)
2. No end effects on dark reaction
3. Weak absorption; $\alpha(Cl_2)R \to 0$
4. Diffusion (radial and longitudinal) is negligible
5. Local rate expression is given by Equation (1A).

Combination of Equation (1A) with Equation (3), which is justified by condition 3, gives

$$-\Omega_{Cl_2} = \frac{2R}{r} K I_{w,\lambda} \alpha_\lambda (Cl_2)^2 \qquad (39)$$

If a filter solution and polychromatic light are used, Equation (39) becomes

$$-\Omega_{Cl_2} = -\frac{d(Cl_2)}{dt} = \frac{2R}{r} K \sigma (Cl_2)^2 \qquad (40)$$

This expression gives the local rate in terms of r and σ.

Conversions for three models were compared:

A. Parabolic velocity profile,

$$v_z = 2\bar{v}_z\left[1 - \left(\frac{r}{R}\right)^2\right] \qquad (41)$$

B. Plug-flow model (no velocity or concentration gradients radially)

C. Diffuse light so that the intensity is constant throughout the reactor at an average value given by the integral of Equation (3) across the radius. For a filter solution, and summed for polychromatic light, this is

$$\bar{I} = 4\sigma \qquad (42)$$

Then the local rate Equation (40) becomes

$$-\Omega_{Cl_2} = -\frac{d(Cl_2)}{dt} = 4\sigma K (Cl_2)^2 \qquad (43)$$

Model A

The average conversion leaving the reactor, in terms of a residence time distribution function ψ, may be written as

$$\bar{x} = \int_{t_{min}}^{\infty} x(t)\, \psi\, dt \qquad (44)$$

$\psi\, dt$ is the volumetric flow rate for a differential annular element divided by the total flow rate Q. Denbigh (*21*) has shown that

$$\psi\, dt = \frac{dQ}{Q} = \frac{(\bar{t})^2}{2t^3} dt \qquad (45)$$

where the local and mean residence time are given by L/v_z and $L/\bar{v}_z$, respectively. The conversion-time relationship $x(t)$, obtained by integrating Equation (40), is

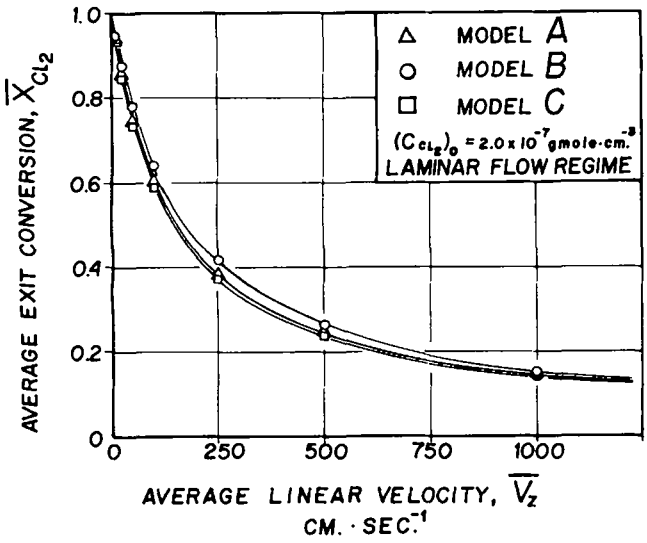

Fig. 9. Parabolic and flat velocity profile models.

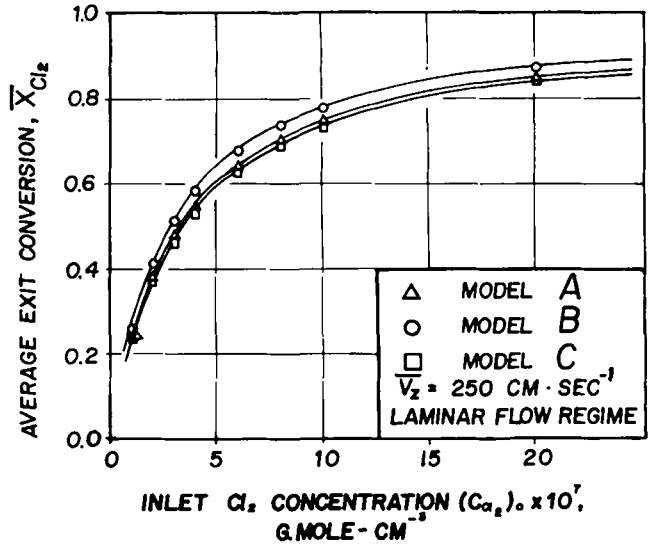

Fig. 10. Parabolic and flat velocity profile models.

$$x(t) = \frac{2K R\sigma (Cl_2)_0 t}{r + 2K R\sigma (Cl_2)_0 t} \qquad (46)$$

Substitution of Equations (45) and (46) in (44) gives

$$\bar{x} = 4K R\sigma (Cl_2)_0 t^2_{min} \int_{t_{min}}^{\infty} \frac{dt}{[r + 2K R\sigma (Cl_2)_0 t] t^2} \qquad (47)$$

where t_{min} applies at the axis of the reactor and is equal to ½ $\bar{t}$. The upper limit of integration is at the wall where $t = \infty$.

For calculations it is more convenient to express Equation (47) in terms of the velocity and reactor length L. Use of Equation (41) for the transformation results in

$$\bar{x} = \frac{\sigma K (Cl_2)_0 L}{(\bar{v}_z)^2} \int_0^{2\bar{v}_z} \frac{v_z\, dv_z}{v_z\left(1 - \frac{v_z}{2\bar{v}_z}\right)^{1/2} + 2\sigma K (Cl_2)_0 L} \qquad (48)$$

Model B

When there are no radial gradients in C and v_z, the rate will be independent of r and given by the integral of Equation (40) from 0 to r, with chlorine constant. The result is

$$-\bar{\Omega}_{Cl_2} = 4K\sigma (\overline{Cl_2})^2 \qquad (49)$$

Substituting this equation in Equation (9) and integrating from 0 to L, we obtain Equation (10), which may be arranged to yield

$$\bar{x} = \frac{K}{K + \frac{\bar{v}_z}{4\sigma (Cl_2)_0 L}} \qquad (50)$$

Model C

In this case the residence time distribution function [Equation (45)] is retained, but $x(t)$ is given by integrating Equation (43) from t_{min} to ∞. The result when substituted in Equation (44) and transformed into velocity, as the independent variable, is

$$\bar{x} = \frac{2K\sigma (Cl_2)_0 L}{(\bar{v}_z)^2} \int_0^{2\bar{v}_z} \frac{v_z\, dv_z}{v_z + 4K\sigma (Cl_2)_0 L} \qquad (51)$$

Results

Equations (48) and (51) were numerically integrated by using the Newton-Cotes five-point formula with a step size of 10^{-6}. The value of K used was that at 30°C., 1.10×10^9 cc./Einstein, obtained in the experimental work for the effect of temperature described earlier. The reactor length was 100 mm. and σ was 2.02×10^{-2} Einsteins/(sec.) (sq. cm.). Figure 9 shows the results when $\bar{x}$ is changed by varying $\bar{v}_z$ from 10 to 1,000 cm./sec. at a constant $(Cl_2)_o$ of 2.0×10^{-7} g.-mole/cc. Figure 10 was obtained by varying $(Cl_2)_o$ from 1.0×10^{-7} to 2.0×10^{-6} at a constant $\bar{v}_z = 250$ cm./sec. The agreement of plug-flow model with model A is reasonably good and better than for nonphotochemical reactions. This is due to the counteracting effects of radial variation in light intensity and of residence time distribution in the photochemical case. Model C shows larger deviations. Note that the inclusion of radial diffusion would reduce the deviation observed for models A and C.

LONGITUDINAL SCALE-UP: COMPARISON WITH DATA

Experimental conversions were measured for $L = 100$ mm. at 30°C. in the 2-mm. I.D. reactor. Data were obtained first at low σ values where differential reactor conditions were obtained. This was done to test the value of K determined from the differential reactor data in the rate vs. temperature series of runs. The experimental and computed results (for models A and B) are shown for the first three runs in Table 5. The agreement achieved does not evaluate the scale-up procedure or models but does substantiate the reproducibility of the differential reactor data.

Then three runs were made at integral reactor conditions with the results given in the last rows of Table 5. The comparison with model A particularly is surprisingly good. The results suggest that for our particular reactor lamp geometry, reaction system, and when end effects are negligible, model A is suitable for longitudinal scale-up. The comparison with model B is not quite as good; errors of 10% were observed.

CONCLUDING DISCUSSION

Incomplete evidence was obtained about the existence of a dark reaction. Acidity was found in the samples from the dark reactor effluent. This could not be attributed to impurities in the water or reagents because these were carefully checked. The same subtracting procedure as described in reference *1* was employed in this study, without concern for the real origin of the acidity. This approach is valid because the extent of the apparent dark reaction was very small.

The chief results of this work are:

1. An increase in chlorine concentration (and corresponding increase in propane and decrease in nitrogen concentrations) from approximately 1 to 4 mole % apparently results in a different reaction mechanism. The intermediate concentration region was not investigated, but rates obtained by extrapolating the second-order equation, valid at low chlorine concentrations, to the higher range were about an order of magnitude high. Two rate equations, both of which include the concentration of propane, were found to fit the rate data at high concentrations.

2. The activation energy for the photochlorination of propane is low, which will simplify reactor design.

3. In a laminar flow photoreactor the effect of the distribution of residence times is less for a second-order reaction than for a conventional reactor.

4. Longitudinal scale-up of a photoreactor was demonstrated under isothermal conditions. A model which takes residence time distribution and radial variation of light intensity into account is satisfactory. It appears that radial scale-up, which can involve changes in the relative importance of heterogeneous and homogeneous processes, will be more difficult. For large-diameter reactors the optical density will not be negligible, thus complicating the integration of the radiation equation.

5. There is evidence that the rate of chlorination increases as the wavelength of the radiation decreases. This suggests that the quantum yield of the primary process is greater for the higher energy corresponding to shorter wavelengths. The effect is not large, and the evidence is not conclusive.

Two important questions remain unanswered. The first is the validity of the steady state hypothesis. This requires two essentially different assumptions in flow reactors. From a reactor design viewpoint it is necessary that mass transport of the activated species, either radially or longitudinally, must be negligible with respect to the conversion of activated species by chemical reaction. Second, from a purely kinetics viewpoint, the concentration of the activated species should be small with respect to the concentrations of reactants and products. An analysis of the criteria for meeting these two assumptions is very difficult for a chain reaction system. The reactor design criterion is intimately related to the diffusivities of the activated species, a subject about which very little is known. The kinetic requirement depends upon a knowledge of the individual rate constants of the initiation, propagation, and termination steps in the reaction sequence. There is some evidence (23) to suggest that the kinetic criterion is more likely to be satisfied for photochemical than for thermal reactions.

The second important question is if heterogeneous termination steps are significant in establishing the overall rate of photochemical reaction. The importance of wall reactions may be evaluated by measuring rates for reac-

TABLE 5. SCALE-UP RESULTS

Run No.	N_{Re}	$\bar{v}_z$, cm./sec.	$(Cl_2)_o$, %	$(C_3H_8)_o$, %	$(N_2)_o$, %	K, cc./Einstein	σ, Einstein/(sec.), (g.-mole)	$\bar{x}$, % exp.	$\bar{x}$, % model A	$\bar{x}$, % model B
S-1	1,236	713	0.56	3.59	95.85	1.10×10^9	0.342×10^{-2}	4.45	4.39	4.55
S-2	1,239	715	0.56	3.58	95.86	1.10×10^9	0.342×10^{-2}	4.52	4.38	4.54
S-3	1,243	717	0.56	3.56	95.88	1.10×10^9	0.342×10^{-2}	4.27	4.39	4.55
S-4	1,232	711	0.56	3.65	95.79	1.10×10^9	2.02×10^{-2}	21.4	20.5	22.0
S-5	1,227	709	0.57	3.63	95.79	1.10×10^9	2.02×10^{-2}	21.2	20.8	22.4
S-6	1,240	715	0.55	3.58	95.87	1.10×10^9	2.02×10^{-2}	19.7	20.1	21.6

$L = 100$ mm.; $T = 30$°C.

tors of different diameters. There have been attempts (*6*, 24, 25) to predict the significance of rupture of chains at the wall, but these depend for their utilization upon a knowledge of rate constants for the individual steps in the chain reaction.

ACKNOWLEDGMENT

The financial support of U.S. Public Health Service, Grant WP AP 00952-01, is gratefully acknowledged. Also the fellowship of the Consejo Nacional de Investigaciones of Argentina granted to Alberto Cassano is appreciated. The authors express their appreciation to the Davis Computer Center NIH Grant No. FR-00009. Thanks are given to J. A. Kent for assistance in the calculations.

NOTATION

A = frequency factor, cc./Einsteins
a = ratio of concentrations of propane and chlorine in reactor feed, Equation (35)
b = ratio of concentrations of nitrogen and chlorine in the feed, Equation (36)
C = concentration also denoted by ( ), g.-mole/cc.
C_x = concentration of oxalic acid
E = apparent activation energy, kcal./g.-mole
F_λ = flux of the light source at wavelength λ, Einsteins/sec.
F_{tot} = total flux of the lamp, Einsteins/sec.
h = Plancks' constant, erg(sec.)/(molecule)
I = light intensity, Einsteins/(sq.cm.)(sec.)
I_w = intensity of radiation from one direction at inside wall of reactor without filter solution [that is, as determined from actinometer measurements by Equation (7)]
$k_1, k_2, \ldots k_6$ = kinetic constants corresponding to individual steps in chain sequence
k'', k''' = kinetic constants as defined by Equations (37) and (38)
k_o = conventional, overall kinetic constant as defined by Equation (1)
k_I and k_{II} = similar constants as defined by Equations (25) and (30)
K = overall kinetic constant independent of light input, defined by Equations (1*A*) and (1*B*), cc./Einstein
K_I and K_{II} = similar constants as defined by Equations (31) and (32)
L = reactor length, cm.
N_{Re} = Reynolds number
Q = volumetric flow rate, cc./sec.
r = radial distance, cm.
r_A = rate of actinometer reaction, g-mole/(sec.)(cc.)
R = reactor radius, cm.
R_g = gas constant, cal./(g.-mole)(°K.)
t = time, sec.
t_{min} = minimum residence time, sec.
$t°$ = temperature, °C.
T = temperature, °K.
V_R = reactor volume, cc.
v_z = axial velocity, cm./sec.
x_A = conversion of oxalic acid in actinometer reaction
x = conversion of chlorine
z = axial distance, cm.

Greek Letters

α = molal absorptivity, defined as $I/I_o = e^{-\alpha C d}$, where d = length of light path, sq.cm./g.-mole
λ = wavelength of light, cm. or Å.
μ = attenuation coefficient (αC), cm^{-1}
ν = frequency of light, $sec.^{-1}$
θ = transmission coefficient of filter solution defined as $\theta = e^{-\mu d}$
Ω_i = rate of formation of species i, g.-mole/(sec.)(cc.)
Φ = quantum efficiency, g.-moles/Einstein
σ = specific rate of energy input, defined by Equation (5), Einsteins/(sec.)(g.-mole)
ψ = time distribution function, $sec.^{-1}$

Subscripts and Superscripts

$\circ$ = activated species or free radical
A = actinometer
i = individual chemical species
o = reactor entrance
( ) = concentration
L = reactor exit
w = reactor wall
r,λ = as subscripts indicates that variable is a function of r and or λ
z = axial direction
t = total
$-$ = average across diameter of reactor or mean concentration

LITERATURE CITED

1. Cassano, A. E., and J. M. Smith, *A.I.Ch.E. J.*, **12**, 1124 (1966).
2. Cassano, A. E., P. L. Silveston, and J. M. Smith, *Ind. Eng. Chem.*, **9**, 18 (1966).
3. Calvert, J. G., and J. N. Pitts, Jr., "Photochemistry," Wiley, New York (1966).
4. Meadows, L. F., and R. M. Noyes, *J. Am. Chem. Soc.*, **82**, 1872 (1960).
5. Hatchard, C. G., and C. A. Parker, *Proc. Royal Soc. (London)* **A.235**, 518 (1956).
6. Leighton, W. G., and G. S. Forbes, *J. Am. Chem. Soc.*, **52**, 3130 (1930).
7. Parker, C. A. *Proc. Royal Soc. (London)*, **220**, 104 (1953).
8. Herr and W. A. Noyes, *J. Am. Chem. Soc.*, **63**, 2052 (1940).
9. Strachan and Blacet, *ibid.*, **77**, 5254 (1955).
10. Fettis, G. C., and J. H. Knox, "Progress in Reaction Kinetics," G. Porter, ed., Vol. 2, Pergamon Press, Oxford (1964).
11. Steacie, E. W. R., "Atomic and Free Radical Reactions," 2 ed., Vol. 2, Reinhold, New York (1954).
12. Knox, J. H., and Nelson, *Trans. Faraday Soc.*, **55**, 937 (1959).
13. Pitzer, E. C., N. E. Gordon, and D. A. Wilson, *J. Am. Chem. Soc.*, **58**, 67 (1936).
14. Davis, W., Jr., *Chem. Rev.*, **40**, 201 (1947).
15. Noyes, W. A., Jr., G. B. Porter, and J. E. Jolley, *Chem. Rev.*, **56**, 49 (1956).
16. Volman, D. H. "Advances in Photochemistry," W. A. Noyes, G. S. Hammond, and J. N. Pitts, ed., Vol. I, Interscience, New York (1963).
17. Gibson, G. E., and N. S. Bayliss, *Phys. Rev.*, **44**, 188 (1933).
18. Chiltz, G., P. Goldfinger, G. Huybrechts, G. Martens, and G. Verbeke, *Chem. Rev.*, **40**, 355 (1963).
19. Stauff, J., and H. J. Schumacher, *Z. Elektrochem.*, **48**, No. 5, 271 (1942).
20. Stauff, J. *ibid.*, **48**, No. 10, 550 (1942).
20A. Noyes, W. A., and P. A. Leighton, "The Photochemistry of Gases," Reinhold, New York (1941).
21. Denbigh, K., "Chemical Reactor Theory," Cambridge Univ. Press, Cambridge (1965).
22. Noyes, R. M., *J. Am. Chem. Soc.*, **73**, 3039 (1951).
23. Benson, S. W., *J. Chem. Phys.*, **20**, No. 10, 1605 (1952).
24. ———, "The Foundations of Chemical Kinetics," McGraw-Hill, New York (1960).
25. Semenoff, N. N., *Acta. Physicochem, U.R.S.S.*, **18**, No. 2-3, 93 (1943).

Manuscript received November 9, 1966; revision received January 8, 1967; paper accepted January 8, 1967.